BIO DESIGN

Selection of differential chirality of (*R*)- and (*S*)-3-hydroxybutyryl-CoA dehydrogenases

Jieun Kim and Kyung-Jin Kim*

Structural and Molecular Biology Laboratory, School of Life Sciences, Kyungpook National University, Daegu 702-701, Korea.
*Correspondence: kkim@knu.ac.kr

(R)- and (S)-3-hydroxybutyryl-CoA dehydrogenases from Ralstonia eutropha H16 play a significant role in the biosynthesis of bioplastics and biofuels. (R)-3-hydroxybutyryl-CoA dehydrogenase (*Re*PhaB) is an enzyme that is involved in the synthetic pathway of polyalkanoates (PHA) which are used to make bioplastics, implant biomaterials, and biofuel. Whereas, (S)-3-hydroxybutyryl-CoA dehydrogenase (*Re*PaaH1) is an enzyme that is involved in the biosynthesis of the n-butanol. Although both these enzymes utilize Acetoacetyl-CoA as a substrate to produce 3-hydroxybutyryl-CoA, the chirality of the final product is different—(R)-3-hydroxybutyryl-CoA by *Re*PhaB and (S)-3-hydroxybutyryl-CoA by *Re*PaaH1. Crystal structures of *Re*PhaB and *Re*PaaH1 show remarkable differences in their structures, oligomeric states, and cofactor specificity. *Re*PhaB forms a tetramer, whereas *Re*PaaH1 forms a dimer. Their cofactor requirements are also different—NADPH and NADH for *Re*PhaB and *Re*PaaH1, respectively. Moreover, their substrate binding modes are also substantially different. Interestingly, both enzymes undergo a conformational change upon binding to acetoaceryl-CoA substrate. In *Re*PhaB, the lid-domain undergoes a large conformational change of about 4.6 Å to form a substrate pocket, whereas only a small structural change is observed in *Re*PaaH1. Comparison of active sites of these enzymes reveals the differences in the position of catalytic residues, which ultimately determines the differential chirality of their products.

INTRODUCTION

Limited fossil fuel availability, greenhouse gas emissions, and the need for increased energy security and diversity has generated a widespread public and scientific awareness towards ecofriendly energy alternatives. A wide range of biofuels as energy substitute can be derived from plant or microbial sources (Demirbas, 2009) out of which ethanol and butanol are two major biofuels with diverse applications are currently in use. Anaerobic bacterium *Clostridium acetobutylicum* efficiently produces *n*-butanol through a carbohydrate catabolic pathway (Inui et al., 2008; Mitchell, 1998). Compared to *n*-butanol, ethanol is a lesser attractive biofuel with low energy efficiency compared to gasoline and high vaporizability (Liu and Qureshi, 2009; Tirado-Acevedo et al., 2010). Biosynthesized *n*-butanol has superior properties over ethanol in that it has a high energy content, low corrosion, increased solubility, and is easier to blend with gasoline (Durre, 2007, 2008; Fischer et al., 2008).

Polyhydroxyalkanoates (PHAs) are generating a considerable amount of interest, which in itself is a family of diverse bio-polyesters. Bacteria produce PHAs via fermentation of either sugars or lipids as a carbon storage material and an energy source (Sudesh et al., 2000). Microorganisms grown in an aqueous solution containing sustainable resources such as starch, glucose, sucrose, and fatty acids carry out biosynthesis of PHAs. Synthetic plastic on the other hand is most commonly derived from petrochemicals. Therefore, PHAs are generally

considered as sustainable and environmentally friendly biopolymers (Ariffin et al., 2010; Lee and Choi, 1999). Efforts have been made over the past decade to find ways in which PHAs can be used to produce bioplastics, fine chemicals, implant biomaterials, medicines, and biofuels (Chen, 2009; Gao et al., 2011; Jian et al., 2010; Keshavarz and Roy, 2010; Mauclaire et al., 2010).

Ralstonia eutropha H16 is a representative bacterial strain used for the PHA biosynthesis. It also encodes an enzyme used for *n*-butanol synthesis. Acetoacetyl-CoA, which serves as a starting molecule for both PHAs and *n*-butanol biosynthesis is produced by condensation of acetyl-CoA after glycolysis by an enzyme called β-ketothiolase (THL, *Re*PhaA) (Figure 1). PHAs are then subsequently biosynthesized by two other key enzymes, NADPH-dependent (R)-3-hydroxybutyryl-CoA dehydrogenase (*Re*PhaB), and PHA synthase (*Re*PhaC) (Peoples and Sinskey, 1989). *n*-Butanol biosynthesis proceeds by converting acetoacetyl-CoA to (S)-3-hydroxybutyryl-CoA which has a different chirality compared to an intermediate of PHAs (i.e. (R)-3-hydroxybutyryl-CoA). Acetoacetyl-CoA is converted to (S)-3-hydroxybutyryl-CoA by *Ralstonia eutropha* (S)-3-hydroxybutyryl-CoA dehydrogenase (*Re*PaaH1) to form an intermediate in n-butanol biosynthesis (Haywood et al., 1988). *Ralstonia eutropha*–derived PaaH1(*Re*PaaH1) is proposed as a homolog of *Clostridium butyricum* 3-hydroxybutyryl-CoA dehydrogenase (*Cb*HBD), which is also thought to be involved in the *n*-butanol
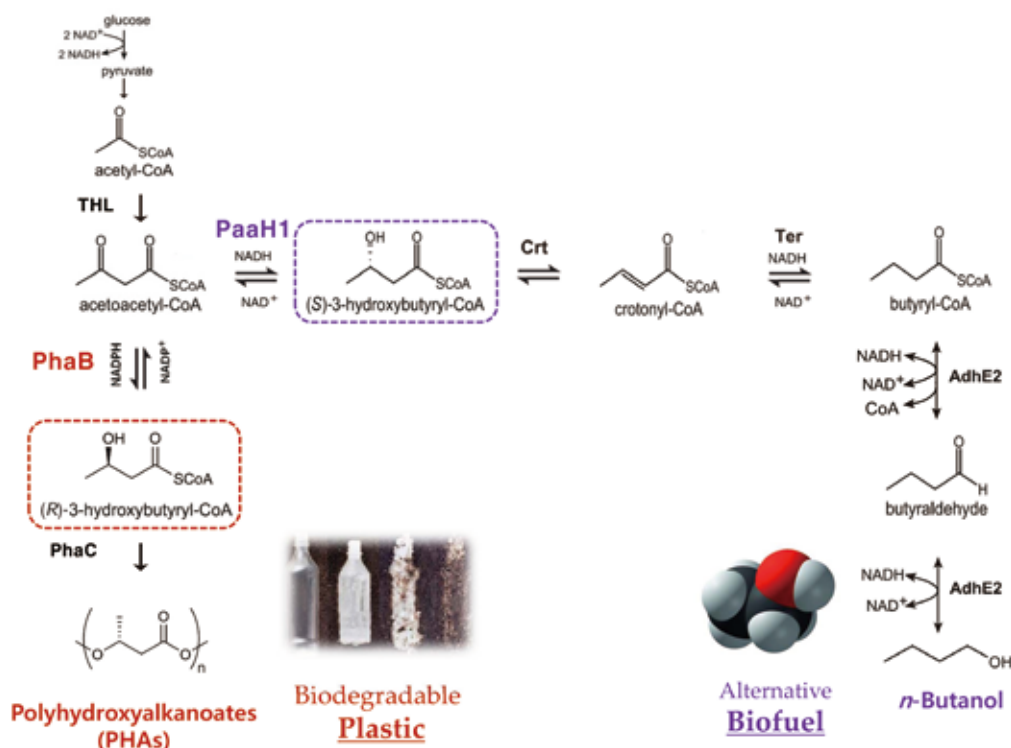
FIGURE 1 | **Biosynthetic pathways of polyhydroxyalkanoates (PHAs) and *n*-butanol.** Biosynthetic pathways for the production of PHAs and *n*-butanol share a common substrate, acetoacetyl-CoA, which is produced by the condensation of Acetyl-CoA. Enzymes and metabolites involved in these pathways are shown and labeled. PhaB and PaaH1 are highlighted with dotted boxes in red and purple, respectively.

biosynthesis (Machado et al., 2012).

It is fascinating to observe that the chirality of a starting molecule plays a crucial role in determining the identity of the final product. It is obvious that the enzymes involved in both the pathways have substrate specificity determined by its chirality. This implies that the host bacteria having certain enzymes that are involved in the synthesis solely determine the final product. Both these enzymes (*Re*PhaB and *Re*PaaH1) which function as reductase of acetoacetyl-CoA and are involved in the synthesis of enantiomers {(R)-3-hydroxybutyryl-CoA and (S)-3-hydroxybutyryl-CoA} show significant differences in their structure (Kim et al., 2014a; Kim et al., 2014b; Kim and Kim, 2014). It is interesting to note that their molecular weights are considerably different (*Re*PhaB, 29 kDa and *Re*PaaH1, 32 kDa), and the fact that there is only 8.54% sequence homology between the two. In this report we are presenting in detail the differences between Ralstonia eutropha (R)- and (S)-3-hydroxybutyryl-CoA dehydrogenases (*Re*PhaB and *Re*PaaH1), enzymes that convert acetoacetyl-CoA to (R)-3-hydroxybutyryl-CoA and (S)-3- hydroxybutyryl-CoA respectively.

STRUCTURAL DIFFERENCES

Crystal structures of *Re*PhaB and *Re*PaaH1 show significant differences in overall fold and oligomeric states for the two proteins. *Re*PhaB exists as a tetramer with four active sites (Kim et al., 2014a). Two of which are on the front and the other two are on the backside with two fold symmetries (Figure 2A). There are two dimeric interfaces, which form a tetramer. One of the interfaces is composed of helices α4, α5 and α4', α5'. They together form a 4-helical bundle through hydrophobic interactions. The other interface is formed between β7 strands from each monomer resulting in the formation of a long β-sheet with 14 β-strands (Kim et al., 2014a). The *Re*PhaB monomer contains a typical Rossmann fold and a substrate binding domain (Figure 2C). The monomeric structure includes a parallel β-sheet composed of seven β-strands flanked on each side by a α helix (Seven β-strands and eight α helices). The core of this structure is made up of two right-handed βαβαβ motifs that are connected by the helix α3. Interestingly, a dip cleft formed in the substrate binding domain is not a common shape. Two helices α4 and α6 extend from the Rossmann fold to form a deep cleft together with the segment consisting of helix α7, loop α7-α8 and helix α8. Since the overall shape of the protruding segments looks like a clamp, it has been named as a Clamp domain (Kim et al., 2014a) . Hereafter, it will be referred to the segment α7, α7-α8 and α8 as a Clamp-lid, and the α4, partial β4-α4, α5-α6 and α6 segment as a Clamp-base.

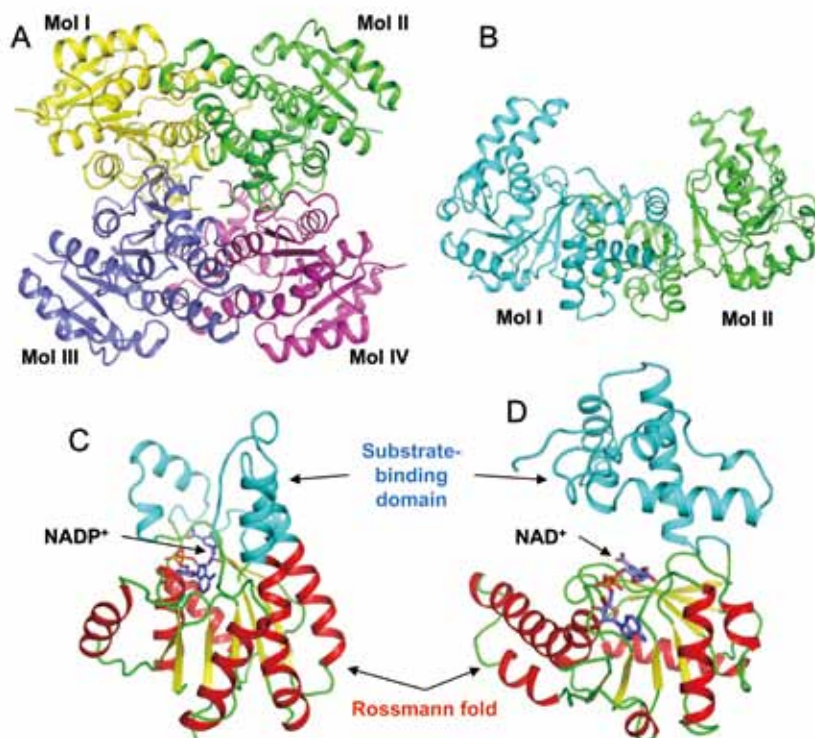*Re*PaaH1 exists as a dimmer with two active sites located in

FIGURE 2 | Overall structures of *Re*PhaB and *Re*PaaH1. (A) Tertameric structure of *Re*PhaB. Four polypeptides are represented by a ribbon diagram in yellow, green, light blue, and magenta. (B) Dimeric structure of *Re*PaaH1. Two polypeptides are represented by a ribbon diagram in green and cyan. (C) Monomeric structure of *Re*PhaB. The Rossmann fold domain and the substrate binding domain are shown in red and cyan, respectively. The bound NADP$^+$ cofactor is shown with a stick model (light blue). (D) Monomeric structure of *Re*PaaH1. The Rossmann fold domain and the substrate binding domains are distinguished using red and cyan, respectively. The bound NAD$^+$ cofactor is presented as a stick model in light blue.

it (figure 2B). The monomer of *Re*PaaH1 contains two separate N- and C-terminal domains (Figure 2D). The N-terminal domain (NTD, residues 1-188) shows a β-α-β fold, and consists of a core containing eight-stranded β-sheet flanked by α-helices. As observed in a typical Rossmann fold, the two parallel β7 and β8 strands exist in a direction to opposite the six parallel strands (β1-β6) of the sheet. A large helix-turn-helix motif (α2 and α3) extends from the β-α-β core, and connects β2 and β3. The C-terminal domain (CTD, residues 189-284), which consists of five α-helices (α8-α12) is mainly involved in the dimerization through hydrophobic interactions with α8 and α9 helices. There are positively charged residues in the cleft between NTD and CTD.

DIFFERENCE IN THE COFACTOR SPECIFICITY

Both *Re*PhaB and *Re*PaaH1 catalyze the reduction of acetoacetyl-CoA utilizing a different cofactor. *Re*PhaB requires NADPH while *Re*PaaH1 uses NADH for its enzymatic action (Kim et al., 2014a; Kim et al., 2014b). The crystal structures of these enzymes with their respective cofactors revealed that both NADP$^+$ and NAD$^+$ bind in the Rossmann fold domain. However,

the cofactor binding modes of these enzymes are substantially different (Figure 3A and B).

Structure of the *Re*PhaB-NADP$^+$ complex shows a distinct similarity to its apoenzyme structure with the root-mean-square deviation of < 0.3 Å. NADP$^+$ binds to the Rossmann fold in much the same way as it does to the other NADP$^+$-binding proteins (Kim et al., 2014a). The nicotinamide ribose moiety is buried by the Clamp domain in such a way that it is located in the deep cleft, whereas the 3'-phosphorylated adenosine moiety of the NADP$^+$ is somewhat exposed at the surface. The part of the enzyme that binds to NADP$^+$ is made up of five loops; β1-α1, β2-α2, partial β4-α4, β5-α5 and β6-α7. However, there is no interaction with the Clamp domain. The nicotinamide ring of NADP$^+$ is positioned in the inner pocket between the Rossmann fold and the Clamp domain, whereas the 3'-phosphate and adenine face outward. NADP$^+$ is bound to the enzyme mainly through hydrogen bonds. The dinucleotide moiety is stabilized by the side chains of Lys157 (NZ) and Tyr153 (OH). The adenine and the 3'-phosphate interact with the side chains of Ser38 (OG), Arg40 (NH2), and Asn61 (OD1) (Figure 3A).

Structure of the RePaaH1-NAD$^+$ complex is similar to that of its apoenzyme, with a root-mean-square deviation of 0.25 Å on 295 Cα atoms (Kim et al., 2014b). As expected, the NAD$^+$ cofactor is bound to the N-terminal Rossmann fold, similar to the binding seen in the other NAD$^+$-binding proteins. The NAD$^+$-binding pocket is composed of five loops (β1-α1, β2-α2, β4-α5, β5-α6, and β6-α7) and one α helix (α5). The Thr13 and Met14 residues in the G-x-G-x-x-G nucleotide-binding motif, which is made up of Gly10-Ala11-Gly12-Thr13-Met14-Gly15 are paired with the two phosphate moieties of NAD$^+$. The nicotinamide ring is positioned near the conserved residue, Asn117. Two ribose rings are stabilized through hydrogen bonding mediated by the side chains of the residues Asp33 and Glu92 (Figure 3B). The adenine moiety of NAD$^+$ is located at the hydrophobic cleft formed by hydrophobic residues such as Tyr77, Ala90, Leu96, and Ile100. The side chain of Tyr77 residue recognizes the adenine moiety by the involvement of hydrogen bonding with the NAD$^+$.

SUBSTRATE BINDING MODE

Both enzymes show structural changes upon binding to their substrate, acetoacetyl-CoA (Kim et al., 2014a; Kim et al., 2014b).
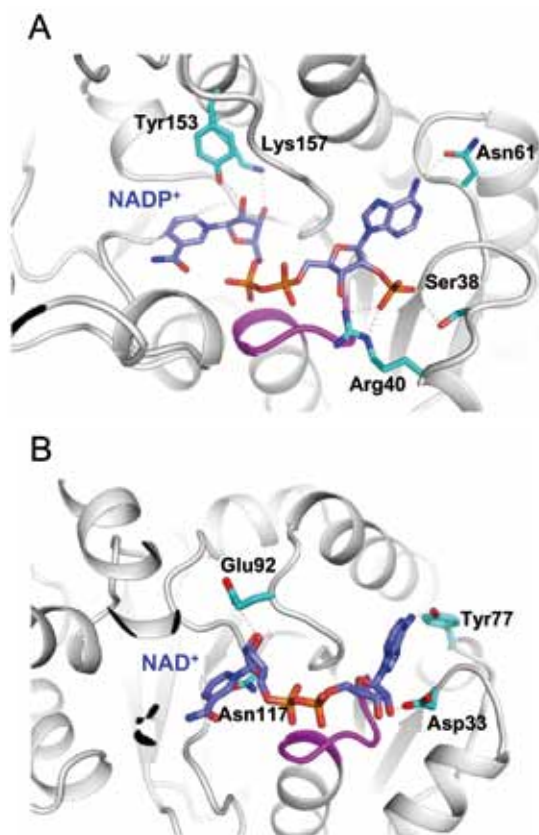
FIGURE 3 | Cofactor-binding modes of *Re*PhaB and *Re*PaaH1.
(A) NADP⁺ binding mode of *Re*PhaB. The *Re*PhaB structure is shown as a cartoon diagram in grey. The bound NADP⁺ cofactor is presented as a stick model in light blue and has been labeled appropriately. Residues involved in NADP⁺ binding are shown as a stick model in cyan. The GxGxxG nucleotide binding motif is shown in magenta. (B) NAD⁺ binding mode of *Re*PaaH1. The *Re*PaaH1 structure is shown as a cartoon diagram in grey. The bound NAD⁺ cofactor is presented as a stick model in light blue and has been labeled appropriately. Residues involved in NAD⁺ binding are shown as a stick model in cyan. The GxGxxG nucleotide binding motif is shown in magenta.

In *Re*PhaB, the substrate acetoacetyl-CoA is bound to the Clamp domain (Figure 4A). The acetoacetyl group positioned near the nicotinamide ring, which acts as an electron donor for the catalytic reduction. Interestingly, conformation of the Clamp domain undergoes structural change about 4.6 Å toward the acetoacetyl-CoA compared to that of the NADP⁺ complex (Kim et al., 2014a). It is clear from the structure that if the Clamp-lid does not undergo a downward structural change, the acetoacetyl-CoA cannot tightly associate with the protein. Therefore, an open-closed conformation of the Clamp-lid is a necessary mechanism for substrate binding in the case of *Re*PhaB. The acetoacetyl-CoA is bound less stringently with the residues in the substrate pocket, while NADP⁺ interacts extensively via hydrogen bonding with the residues in the cleft region of *Re*PhaB (Kim et al., 2014a). The carbonyl groups of the acetoacetyl moiety interact via hydrogen bonding to the nitrogen atom of the Q150
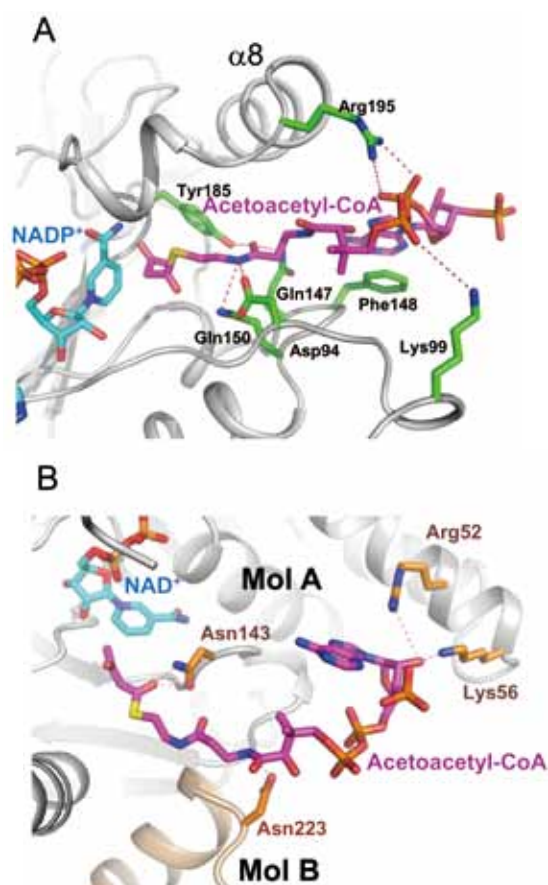
FIGURE 4 | Substrate-binding modes of *Re*PhaB and *Re*PaaH1.
(A) Acetoacetyl-CoA binding mode of *Re*PhaB. The *Re*PhaB structure is shown as a cartoon diagram in grey. The bound acetoacetyl-CoA and NADP⁺ are presented as a stick model in magenta and cyan, respectively. Residues involved in binding of the acetoacetyl-CoA are shown as a stick model in green. The α-8 helix that undergoes structural change upon binding of the substrate is labeled. (B) Acetoacetyl-CoA binding mode of *Re*PaaH1. The *Re*PaaH1 structure is shown as a cartoon diagram in grey. The bound acetoacetyl-CoA and NAD⁺ are presented as a stick model in magenta and cyan, respectively. Residues involved in the binding of acetoacetyl-CoA are shown as a stick model in green. The neighboring polypeptide is shown in salmon color and has been labeled.

side chain. The pantotheine group is stabilized via hydrogen bonding with the side chains of the residues Gln147, Gln150, and Tyr185 and via van der Waals interactions with the residues Val 95, Val96, and Tyr185. There is a water-mediated interaction between β-phosphate and Lys99, and the two phosphate groups in the 3'-phosphate adenosine moiety that are bound to the NH1 and NH2 groups of the Arg195 residue. Additionally, the adenine ring, which is stacked above the Phe148 residue, is stabilized by π-π interaction. Acetoacetyl-CoA can perfectly enter in the central cleft in the closed Clamp-lid conformation, but not in the open form. This implies that the Clamp-lid is responsible for both the recognition and the stabilization of the substrate during enzymatic catalysis. Therefore the Clamp domain is involved in positioning the substrate in the cleft region and in stabilizing the
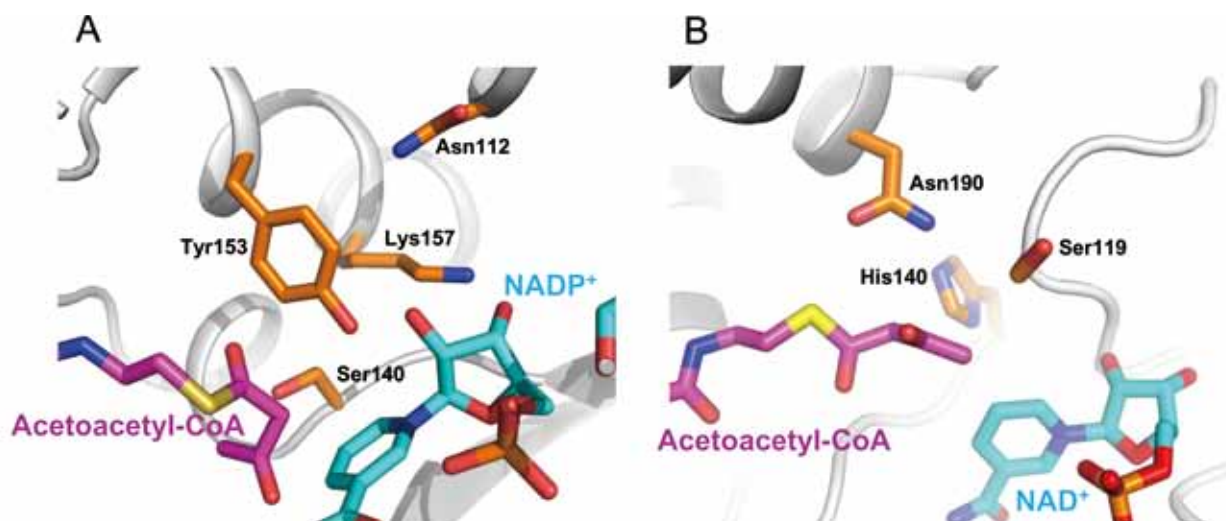
FIGURE 5 | Catalytic sites of *Re*PhaB and *Re*PaaH1. (A) Catalytic site of *Re*PhaB. Residues involved in the enzyme catalysis are presented as a stick model in orange. The bound acetoacetyl-CoA and NADP$^+$ are presented as a stick model in magenta and cyan, respectively. (B) Catalytic site of *Re*PaaH1. Residues involved in the enzyme catalysis are presented as a stick model in orange. The bound acetoacetyl-CoA and NAD$^+$ are presented as a stick model in magenta and cyan, respectively.

substrate conformation.

Unlike in *Re*PhaB, only a small structural change is observed in *Re*PaaH1 upon binding to its substrate. The positions of the two domains after binding to acetoacetyl-CoA substrate are quite similar to those of the apoenzyme, with a root-mean-square deviation of 0.31 Å. This suggests that *Re*PaaH1, unlike *Re*PhaB, does not undergo a large domain shift upon substrate binding (Kim et al., 2014b). The acetoacetyl-CoA substrate in *Re*PhaB is located within the deep cleft between the NTD and CTD. Mainly the side chain of Asn143 as well as the side chain of Asn223 from the other subunit of the dimer stabilizes the pantothenic moiety of the substrate through hydrogen bonding interactions. The acetoacetyl moiety in its binding pocket positioned near the nicotinamide ring of the cofactor NADP$^+$, which acts as an electron donor for the catalytic reduction (Figure 4B). Even though two positively charged residues Arg52 and Lys56 seem to be involved in the hydrogen bonding with the adenosine moiety, its electron density map is not clear implying that the adenosine diphosphate moiety may not be fully stabilized.

DIFFERENCE IN THE ACTIVE SITE

*Re*PhaB and *Re*PaaH1 catalyze the reduction reaction of acetoacetyl-CoA. The reduction mechanism requires a transfer of hydrogen from nicotinamide ring of NADPH or NADH to acetoacetyl-CoA (Kim et al., 2014a; Kim et al., 2014b). In both the cases, catalytic residues are positioned in proximity to the substrate and nicotinamide ring of the cofactor for the proton relay mechanism.

Chirality of the 3-hydroxubutyrate product is determined by the position of the serine residue relative to the position of the C3 carbon of acetoacetyl-CoA and the nicotinamide ring of the cofactor. The direction in which the hydrogen is added to C3 carbon of acetoacetyl-CoA determines the chirality of the product. In *Re*PhaB, hydrogen is added to the *Si*-face of a C3 carbon of the carbonyl group to form a (R)-3-hydroxybutyrate product. However, in case of *Re*PaaH1, hydrogen is added to the *Re*-face of a C3 carbon of the carbonyl group and (S)-compound is produced.

In *Re*PhaB enzyme, the catalytic residues Ser140, Tyr153, Lys157, and Asn112 are involved in the reduction mechanism. Oxygen of the C3 carbonyl group of acetoacetyl-CoA is located near Ser140 exposing the Si-face of the C3 carbonyl group to nicotinamide ring of NADPH (Figure 5A). NADPH donates a hydride to Si-face of the C3 carbon of the substrate, and a proton is transferred to the oxygen from the hydroxyl group of Tyr153. The Tyr153 proton is then replenished by the proton relay system through Lys157 and a chain of water molecules that communicate with the solvent. Asn112 is a key to the integrity of the water network and should be regarded as a bone fide active site residue (Oppermann et al., 2003), it does not directly participate in the catalysis but plays a crucial role by participating in the proton wire.

In *Re*PaaH1 enzyme, the catalytic residues Ser119, Asn190, and His140 are involved in the reduction mechanism. Positions of Ser119, nicotinamide ring of NADH and C3 carbonyl group of acetoacetyl-CoA in *Re*PaaH1 are different from that of *Re*PhaB (Figure 5B). Oxygen of the C3 carbonyl group of acetoacetyl-CoA is positioned near Ser119 exposing the *Re*-face of the C3 carbonyl group to nicotinamide ring of NADH. *Re*-face of the C3 carbon of carbonyl group adds hydrogen from NADH replenishing the proton deficiency by a relay mechanism of His140, Asn190 and water molecules in the solvent producing a

(S)-3-hydroxubutyrate product.

AUTHOR INFORMATION

The authors declare no potential conflicts of interest.

———————

REFERENCES

Ariffin, H., Nishida, H., Hassan, M. A., and Shirai, Y. (2010). Chemical recycling of polyhydroxyalkanoates as a method towards sustainable development. *Biotechnol J* **5**, 484-492.

Chen, G.Q. (2009). A microbial polyhydroxyalkanoates (PHA) based bio- and materials industry. *Chemical Society Reviews* **38**, 2434-2446.

Demirbas, A. (2009). Biorefineries: Current activities and future developments. *Energy Conversion and Management* **50**, 2782-2801.

Durre, P. (2007). Biobutanol: an attractive biofuel. *Biotechnol J* **2**, 1525-1534.

Durre, P. (2008). Fermentative butanol production - Bulk chemical and biofuel. *Incredible Anaerobes: From Physiology to Genomics to Fuels* **1125**, 353-362.

Fischer, C.R., Klein-Marcuschamer, D., and Stephanopoulos, G. (2008). Selection and optimization of microbial hosts for biofuels production. *Metabolic Engineering* **10**, 295-304.

Gao, X., Chen, J.C., Wu, Q., and Chen, G.Q. (2011). Polyhydroxyalkanoates as a source of chemicals, polymers, and biofuels. *Current Opinion in Biotechnology* **22**, 768-774.

Haywood, G.W., Anderson, A.J., Chu, L., and Dawes, E.A. (1988). The role of NADH- and NADPH-linked acetoacetyl-CoA reductases in the poly-3-hydroxybutyrate synthesizing organism Alcaligenes eutrophus. *FEMS Microbiology Letters* **52**, 259-264.

Inui, M., Suda, M., Kimura, S., Yasuda, K., Suzuki, H., Toda, H., Yamamoto, S., Okino, S., Suzuki, N., and Yukawa, H. (2008). Expression of Clostridium acetobutylicum butanol synthetic genes in Escherichia coli.

Applied microbiology and biotechnology **77**, 1305-1316.

Jian, J., Zhang, S.Q., Shi, Z.Y., Wang, W., Chen, G.Q., and Wu, Q. (2010). Production of polyhydroxyalkanoates by Escherichia coli mutants with defected mixed acid fermentation pathways. *Appl Microbiol Biotechnol* **87**, 2247-2256.

Keshavarz, T., and Roy, I. (2010). Polyhydroxyalkanoates: bioplastics with a green agenda. *Current Opinion in Microbiology* **13**, 321-326.

Kim, J., Chang, J.H., Kim, E.J., and Kim, K.J. (2014a). Crystal structure of (R)-3-hydroxybutyryl-CoA dehydrogenase PhaB from Ralstonia eutropha. *Biochem Biophys Res Commun* **443**, 783-788.

Kim, J., Chang, J.H., and Kim, K.J. (2014b). Crystal structure and biochemical properties of the (S)-3-hydroxybutyryl-CoA dehydrogenase PaaH1 from Ralstonia eutropha. *Biochem Biophys Res Commun* **448**, 163-168.

Kim, J., and Kim, K.J. (2014). Cloning, expression, purification, crystallization and X-ray crystallographic analysis of the (S)-3-hydroxybutyryl-CoA dehydrogenase PaaH1 from Ralstonia eutropha H16. *Acta Crystallogr F Struct Biol Commun* **70**, 955-958.

Lee, S.Y., and Choi, J.I. (1999). Production and degradation of polyhydroxyalkanoates in waste environment. *Waste Management* **19**, 133-139.

Liu, S.Q., and Qureshi, N. (2009). How microbes tolerate ethanol and butanol. *New Biotechnology* **26**, 117-121.

Machado, H.B., Dekishima, Y., Luo, H., Lan, E.I., and Liao, J.C. (2012). A selection platform for carbon chain elongation using the CoA-dependent pathway to produce linear higher alcohols. *Metab Eng* **14**, 504-511.

Mauclaire, L., Brombacher, E., Bunger, J.D., and Zinn, M. (2010). Factors controlling bacterial attachment and biofilm formation on medium-chain-length polyhydroxyalkanoates (mcl-PHAs). *Colloids Surf B Biointerfaces* **76**, 104-111.

Mitchell, W.J. (1998). Physiology of carbohydrate to solvent conversion by clostridia. *Adv Microb Physiol* **39**, 31-130.

Oppermann, U., Filling, C., Hult, M., Shafqat, N., Wu, X., Lindh, M., Shafqat, J., Nordling, E., Kallberg, Y., Persson, B., and Jornvall, H. (2003). Short-chain dehydrogenases/reductases (SDR): the 2002 update. *Chem Biol Interact* **143-144**, 247-253.

Peoples, O.P., and Sinskey, A.J. (1989). Poly-beta-hydroxybutyrate (PHB) biosynthesis in Alcaligenes eutrophus H16. Identification and characterization of the PHB polymerase gene (phbC). *J Biol Chem* **264**, 15298-15303.

Sudesh, K., Abe, H., and Doi, Y. (2000). Synthesis, structure and properties of polyhydroxyalkanoates: biological polyesters. *Progress in Polymer Science* **25**, 1503-1555.

Tirado-Acevedo, O., Chinn, M.S., and Grunden, A.M. (2010). Production of biofuels from synthesis gas using microbial catalysts. *Adv Appl Microbiol* **70**, 57-92.